Crystal Engineering of Nonlinear Optical Materials Based on Interpenetrated Diamondoid Coordination Networks

Owen R. Evans and Wenbin Lin*

Department of Chemistry, Venable and Kenan Laboratories CB#3290, University of North Carolina, Chapel Hill, North Carolina 27599

Received April 3, 2001. Revised Manuscript Received June 4, 2001

Zinc(II) and cadmium(II) coordination networks with *p*-pyridinecarboxylate bridging ligands, Zn(4-pyridylacrylate)$_2$ **(3)**, [Cd(4-pyridylacrylate)$_2$]·H_2O **(4)**, Cd[4-(4-pyridyl)benzoate]$_2$·H_2O **(5)**, and [$Zn_2(\mu$-OH)(4-pyridylbenzoate)$_3$]·EtOH **(6),** have been synthesized under hydro(solvo)thermal conditions. Despite very different metal coordination environments, compounds **3**, **4**, and **6** all adopt 5-fold interpenetrated diamondoid structures, while compound **5** adopts a 7-fold interpenetrated diamondoid structure. The use of unsymmetrical *p*-pyridinecarboxylate bridging ligands in **3**−**5** has ensured their acentricity. Compounds **3**−**5** show significant powder second-harmonic-generation efficiencies. Compound **6**, however, adopts a centrosymmetric structure because of the presence of symmetrical bis[4-(4-pyridyl)-benzoate] double bridges. Compounds **4**−**6** also exhibit open channels that are occupied by removable included guest molecules. The present work illustrates the potential of rational synthesis of NLO-active acentric solids based on interpenetrated diamondoid structures. Crystal data for **3**: monoclinic space group *Cc*, $a = 10.352(1)$ Å, $b = 22.413(2)$ Å, $c = 8.319(1)$ Å, $\beta = 126.149(1)°$, and $Z = 4$. Crystal data for **4**: monoclinic space group *Cc*, $a = 12.013(1)$ Å, $b = 22.344(1)$ Å, $c = 7.774(1)$ Å, $\beta = 123.509(1)°$, and $Z = 4$. Crystal data for **5**: monoclinic space group *Ia*, $a = 22.92(2)$ Å, $b = 28.74(2)$ Å, $c = 23.00(2)$ Å, $\beta = 94.908(8)°$, and $Z = 4$. Crystal data for **6**: monoclinic space group $P2_1/n$, $a = 22.028(1)$ Å, $b = 6.780(1)$ Å, $c = 24.399(1)$ Å, $\beta = 105.096(1)°$, and $Z = 4$.

Introduction

The future of photonics technology in which information is acquired, processed, and transmitted using photons is dependent upon the design and characterization of materials that exhibit second-order nonlinear optical (NLO) properties.[1] There has been intensive research on organic second-order NLO materials such as electric-field-poled polymers[2] and acentric Langmuir−Blodgett and self-assembled multilayer thin films[3] over the past couple of decades. To date, however, only inorganic second-order NLO materials such as lithium niobate and potassium dihydrogen phosphate (KDP) have found practical applications in electrooptic devices. The most challenging hurdle to the practical applications of organic NLO materials lies in the requirement of noncentrosymmetric arrangement of highly dipolar molecules in the bulk. This is because the third rank tensor χ^2 will vanish in a centrosymmetric environment.[4] The construction of acentric bulk materials containing NLO chromophores continues to defy conventional synthetic methodologies and presents a significant challenge to synthetic chemists and materials scientists.[5]

In light of recent success in the construction of potentially useful metal−organic frameworks using strong and highly directional metal−ligand coordination bonds,[6] we have decided to explore the rational synthesis of acentric metal−organic coordination networks that can be used for second-order NLO applications.[7] The key to our synthetic strategies lies in the utilization of metal−ligand coordination bonds to counteract un-

(1) Waldrop, M. M. *Science* **1993**, *259*, 456.

(2) Moerner, W. E.; Silence, S. M. *Chem. Rev.* **1994**, *94*, 127−155. (b) Drost, K. J.; Jen, A. K.-Y., Rao, V. P. *ChemTech* **1995**, *25* (9), 16−25. (c) Dalton, L. R.; Harper, A. W.; Wu, B.; Ghosn, R.; Laquindanum, J.; Liang, Z.; Hubbel, A.; Xu, C. *Adv. Mater.* **1995**, *7*, 519−540. (d) Burland, D. M.; Miller, R. D.; Walsh, C. A. *Chem. Rev.* **1994**, *94*, 31−75. (e) Dalton, L. R.; Harper, A. W.; Ghosn, R.; Steier, W. H.; Ziari, M.; Fetterman, H.; Shi, Y.; Mustacich, R. V.; Jen, A. K.-Y.; Shea, K. J. *Chem. Mater.* **1995**, *7*, 1060−1081.

(3) Marks, T. J.; Ratner, M. A. *Angew. Chem., Int. Ed. Engl.* **1995**, *34*, 155−173. (b) Lin, W.; Lin, W.; Wong, G. K.; Marks, T. J. *J. Am. Chem. Soc.* **1996**, *118*, 8034−8042. (c) Lundquist, P. M.; Lin, W.; Zhou, H.; Hahn, D. N.; Yitzchaik, S.; Marks, T. J.; Wong, G. K. *Appl. Phys. Lett.* **1997**, *70*, 1941−1943. (d) Katz, H. E.; Wilson, W. L.; Scheller, G. *J. Am. Chem. Soc.* **1994**, *116*, 6636−6640.

(4) Zyss, J. *Molecular Nonlinear Optics: Materials, Physics, and Devices*; Academic Press: New York, 1993. (b) Agulló-López, F.; Cabrera, J. M.; Agulló-Rueda, F. *Electrooptics: Phenomena, Materials and Applications*; Acdemic Press: New York, 1994.

(5) Desiraju, G. R. *Crystal Engineering: The Design of Organic Solids*; Elsevier: New York, 1989. (b) Lehn, J.-M. *Supramolecular Chemistry*: *Concepts and Perspectives*; VCH Publishers: New York, 1995.

(6) Zaworotko, M. J. *Chem. Soc. Rev.* **1994**, 283−288. (b) Hagrman, P. J.; Hagrman, D.; Zubieta, J. *Angew. Chem., Int. Ed. Engl.* **1999**, *38*, 2638−2684. (c) Yaghi, O. M.; Li, H.; Davis, C.; Richardson, D.; Groy, T. L. *Acc. Chem. Res.* **1998**, *31*, 474−484. (d) Munakata, M.; Wu, L. P.; Kuroda-Sowa, T. *Adv. Inorg. Chem.* **1999**, *46*, 173−304. (e) Janiak, C. *Angew. Chem., Int. Ed. Engl.* **1997**, *36*, 1431.

(7) Evans, O. R.; Xiong, R.-G.; Wang, Z.; Wong, G. K.; Lin, W. *Angew. Chem., Int. Ed. Engl.* **1999**, *38*, 536−538. (b) Lin, W.; Wang, Z.; Ma, L. *J. Am. Chem. Soc.* **1999**, *121*, 11249−11250. (c) Lin, W.; Evans, O. R.; Xiong, R.-G.; Wang, Z. *J. Am. Chem. Soc.* **1998**, *120*, 13272−13273. (d) Lin, W.; Ma, L.; Evans, O. R. *Chem. Commun.* **2000**, 2263−2264.

10.1021/cm010301n CCC: $20.00
Published on Web 06/30/2001

favorable centric interactions such as dipole−dipole repulsions. It is now well-established that metal−organic frameworks have a high tendency to adopt diamondoid network topologies.[8] Moreover, as exemplified by the prototypical NLO material KDP,[9] diamondoid networks represent an interesting structural motif for the construction of acentric solids because they are not predisposed to pack in centric space groups owing to the lack of inversion centers on each tetrahedral connecting point. We surmise that an intrinsically acentric diamond net will arise if unsymmetrical bridging ligands are used to link tetrahedrally connected metal centers. Furthermore, the use of unsymmetrical, bifunctional bridging ligands (e.g., pyridinecarboxylates) also introduces the electronic asymmetry (push−pull effects) that is essential for second-order optical nonlinearity. However, metal−organic diamondoid networks tend to interpenetrate to fill the voids generated within a single diamond net, which could potentially introduce an inversion center and complicate the crystal engineering of acentric solids based on diamondoid networks. We report here the rational synthesis of acentric solids based on metal−organic diamondoid networks with an odd number of interpenetrating nets. A small portion of this work has been previously communicated.[7a]

Experimental Section

Materials and Methods. 4-Bromopyridine hydrochloride was obtained from TCI America, while all of the other chemicals were obtained from Aldrich. All of the chemicals were used without further purification. *Caution: $Zn(ClO_4)_2 \cdot 6H_2O$ and $Cd(ClO_4)_2 \cdot 6H_2O$ are potentially explosive and should be used with care!* Thermogravimetric analyses were performed in air at a scan speed of 10 °C/min on a Shimadzu TGA-50 TG analyzer. ^1H and $^{13}C\{^1H\}$ NMR spectra were taken on a Varian Inova spectrometer at 400 and 100 MHz, respectively. Infrared spectra were measured either with KBr pellets or with a chloroform solution on a Perkin-Elmer Paragon 1000 FT-IR spectrometer. X-ray powder diffraction (XRPD) data were recorded on a Rigaku RU300 diffractometer at 60 kV and 300 mA for Cu Kα ($\lambda = 1.5418$ Å), with a scan speed of 2°/min and a step size of 0.02° in 2θ. The calculated XRPD patterns were produced using the SHEXTL-XPOW program and single-crystal reflection data. All of the spectroscopic data for compounds **1**−**6** can be found in the Supporting Information.

Kurtz powder second-harmonic-generation (SHG) measurements were performed on ground samples of crystalline **3**−**6**.[10] The powder samples have been sized to a particle size of 76 ± 13 μm. The fundamental wavelength of 1064 nm from a Nd:YAG laser was used. The powder second-harmonic signals were compared to that of α-quartz to determine the relative SHG efficiencies of **3**-**6**.

Synthesis of Ethyl 4-Pyridylacrylic Ester (1). A mixture of 4-bromopyridine hydrochloride (4.0 g, 20.5 mmol) and ethyl acrylate (2.053 g, 20.5 mmol) in 20 mL of triethylamine and 50 mL of dimethylformamide was refluxed in the presence of palladium(II) acetate (0.050 g, 0.22 mmol) and tri-*o*-tolylphosphine (0.100 g, 0.33 mmol) for 12 h. After removal of the volatiles under reduced pressure, the residue was dissolved in 150 mL of ethyl acetate and washed twice with 50 mL of water. The organic layer was dried over $MgSO_4$ and evaporated to dryness. Silica gel chromatography eluting with a mixture of ethyl acetate and hexanes (1:1, v/v) afforded 3.471 g of pure **1** (yield: 89%).

Synthesis of 4-(4-Pyridyl)benzonitrile (2). A mixture of 4-(trimethylstannyl)pyridine[11] (2.128 g, 8.8 mmol) and 4-bromobenzonitrile (2.013 g, 11 mmol) in 15 mL of dry toluene was refluxed in the presence of tetrakis(triphenylphosphine)-palladium for 18 h. Toluene was removed under reduced pressure; the residue was dissolved in 150 mL of ethyl acetate and washed twice with 50 mL of water. The organic layer was dried over $MgSO_4$ and evaporated to dryness. Silica gel chromatography eluting with a mixture of ethyl acetate and hexanes (3:1, v/v) afforded 1.38 g of pure **2** (yield: 87%).

Synthesis of Zn(4-pyridylacrylate)$_2$ (3). A heavy-walled Pyrex tube containing a mixture of $Zn(ClO_4)_2 \cdot 6H_2O$ (0.186 g, 0.5 mmol) and ethyl 4-pyridylacrylic ester (0.177 g, 1 mmol) in methanol (0.4 mL) and water (0.1 mL) was frozen, sealed under vacuum, and placed inside an oven at 95 °C. Colorless prismatic crystals were obtained after 24 h of heating. Yield: 0.063 g (35%). Anal. Calcd (found) for $C_{16}H_{12}N_2O_4Zn$: C, 53.1 (52.5); H, 3.34 (3.75); N, 7.75 (7.59). Thermogravimetric analysis of **3** revealed no weight loss until the onset decomposition temperature of 360 °C.

Synthesis of [Cd(4-pyridylacrylate)$_2$]·H$_2$O (4). A heavy-walled Pyrex tube containing a mixture of $Cd(ClO_4)_2 \cdot 6H_2O$ (0.22 g, 0.5 mmol) and *trans*-4-pyridylacrylic acid (0.15 g, 1 mmol) in ethanol (0.4 mL) was frozen, sealed under vacuum, and placed inside an oven at 130 °C. Colorless prismatic crystals were obtained after 48 h of heating. Yield: 0.11 g (53%). Anal. Calcd (found) for $CdC_{16}H_{14}O_5N_2$: C, 45.0 (44.6); H, 2.83 (3.16); N, 6.56 (6.49). Thermogravimetric analysis of **4** revealed a 4.6% weight loss by 75 °C, corresponding to the loss of one water molecule per formula unit (4.2%).

Synthesis of Cd[4-(4-pyridyl)benzoate]$_2$·H$_2$O (5). A mixture of $Cd(NO_3)_2 \cdot 4H_2O$ (0.039 g, 0.125 mmol) and 4-(4-pyridyl)benzonitrile (0.043 g, 0.25 mmol) was thoroughly mixed with ethanol (0.7 mL), pyridine (0.4 mL), and deionized water (0.4 mL) in a heavy-walled Pyrex tube. The tube was frozen under liquid nitrogen, sealed, and placed inside an oven at 140 °C. After 7 days of heating, rectangular colorless crystals were obtained. Yield: 0.043 g (65.4%). Anal. Calcd (found) for $C_{24}H_{18}CdN_2O_5$: C, 54.7 (54.2); H, 3.44 (3.01); N, 5.32 (5.40).

Synthesis of [Zn$_2$(μ-OH)[4-(4-pyridyl)benzoate]$_3$]·EtOH (6). A heavy-walled Pyrex tube containing a mixture of $Zn(ClO_4)_2 \cdot 6H_2O$ (0.023 g, 0.0625 mmol) and 4-(4-pyridyl)benzonitrile (0.032 g, 0.188 mmol) in ethanol (0.4 mL), water (0.1 mL), and pyridine (0.1 mL) was frozen, sealed under vacuum, and placed inside an oven at 130 °C. Colorless needlelike crystals were obtained after 6 days of heating. Yield: 0.011 g (44%). Anal. Calcd (found) for $C_{38}H_{31}N_3O_8Zn_2$: C, 57.9 (54.1); H, 3.96 (3.52); N, 5.33 (5.37). Several samples have been tried; the carbon content was always lower than expected. Thermogravimetric analysis of **6** revealed a 5.3% weight loss by 110 °C, corresponding to the loss of one ethanol molecule per formula unit (5.8%).

X-ray Structure Determinations. Data collections for compounds **3**−**6** were carried out on a Siemens SMART system equipped with a CCD detector using Mo Kα radiation with

(8) Proserpio, D. M.; Hoffmann, R.; Preuss, P. *J. Am. Chem. Soc.* **1994**, *116*, 9634. (b) Batten, S. R.; Robson, R. *Angew. Chem., Int. Ed. Engl.* **1998**, *37*, 1461. (c) Zaworotko, M. J. *Chem. Soc. Rev.* **1994**, 283. (d) Lopez, S.; Kahraman, M.; Harmata, M.; Keller, S. W. *Inorg. Chem.* **1997**, *36*, 6138. (e) Blake, A. J.; Champness, N. R.; Chung, S. S. M.; Li, W.-S.; Schröder, M. *Chem. Commun.* **1997**, 1005. (f) Carlucci, L.; Ciani, G.; Proserpio, D.; Sironi, A. *Chem. Commun.* **1994**, 2755. (g) MacGillivray, L. R.; Subramanian, S.; Zaworotko, M. J. *Chem. Commun.* **1994**, 1325. (h) Michaelides, A.; Kiritsis, V.; Skoulika, S.; Aubry, A. *Angew. Chem., Int. Ed. Engl.* **1993**, *32*, 1495. (i) Hirsch, K. A.; Venkataraman, D.; Wilson, S. R.; Moore, J. S.; Lee, S. *Chem. Commun.* **1995**, 2199. (j) Hirsch, K. A.; Wilson, S. R.; Moore, J. S. *Chem. Eur. J.* **1997**, *3*, 765. (k) Hirsch, K. A.; Wilson, S. R.; Moore, J. S. *Inorg. Chem.* **1997**, *36*, 2960. (l) Munakata, M.; Wu, L. P.; Yamamoto, M.; Kuroda-Sowa, T.; Maekawa, M. *J. Am. Chem. Soc.* **1996**, *118*, 3117. (m) Sinzger, K.; Hünig, S.; Jopp, M.; Bauer, D.; Bietsch, W.; von Schütz, J. U.; Wolf, H. C.; Kremer, R. K.; Metzenthin, T.; Bau, R.; Khan, S. I.; Lindbaum, A.; Langauer, C. L.; Tillmanns, E. *J. Am. Chem. Soc.* **1993**, *115*, 7696. (n) Cromer, D. T.; Larson, A. C. *Acta Crystallogr.* **1972**, *B28*, 1052.

(9) Endo, S.; Chino, T.; Tsuboi, S.; Koto, K. *Nature* **1989**, *340*, 452−455.

(10) Kurtz, S. K.; Perry, T. T. *J. Appl. Phys.* **1968**, *39*, 3798−3813.

(11) Yammamoto, A.; Yanagi, *Chem. Pharm. Bull.* **1982**, *30*, 1731−1737.

Table 1. Data for the X-ray Diffraction of 3−6[a]

	chemical formula			
	$ZnC_{16}H_{12}N_2O_4$ (**3**)	$CdC_{16}H_{14}N_2O_5$ (**4**)	$CdC_{24}H_{18}N_2O_5$ (**5**)	$Zn_2C_{38}H_{31}N_3O_8$ (**6**)
crystal system	monoclinic	monoclinic	monoclinic	monoclinic
a, Å	10.352(1)	12.013(1)	22.92(2)	22.028(1)
b, Å	22.413(2)	22.344(1)	28.74(2)	6.780(1)
c, Å	8.319(1)	7.774(1)	23.00(2)	24.399(1)
β, deg	126.149(1)	123.509(1)	94.908(8)	105.096(1)
V, Å^3	1558.5(2)	1739.9(1)	15093(19)	3518.3(4)
Z	4	4	4	4
formula wt	361.67	426.70	526.82	773.24
space group	*Cc* (No. 9)	*Cc* (No. 9)	*Ia* (No. 9)	$P2_1/n$ (No. 14)
T, °C	−100 (2)	−75 (1)	−70(2)	−80(2)
λ (Mo Kα), Å	0.71073	0.71073	0.71073	0.71073
ρ_{calc}, g/cm^3	1.54	1.63	1.62	1.49
μ, cm^{-1} (Mo Kα)	16.0	12.8	10.5	14.2
no. of unique reflections	2969	3533	25025	8379
no. of obs refs [$I > 2\sigma(I)$]	2808	3466	15676	4518
N_{para}	256	217	1078	466
min and max residual density, e/Å^3	−0.53, 0.44	−1.87, 0.94	−1.05, 1.52	−0.52, 1.09
R1	0.026	0.054	0.067	0.061
*w*R2	0.066	0.144	0.156	0.185
goodness of fit	1.04	1.07	1.10	1.00
flack parameter	0.00(2)	0.00(6)	0.46(3)	N/A

[a] $R1 = \sum||F_o| - |F_c||/\sum|F_o|$; $wR2 = [\sum[w(F_o^2 - F_c^2)^2]/\sum[w(F_o^2)^2]]^{1/2}$; $GOF = [\sum[w(F_o^2 - F_c^2)^2]/(\text{no. of reflections} - \text{no. of parameters})]^{1/2}$.

Scheme 1

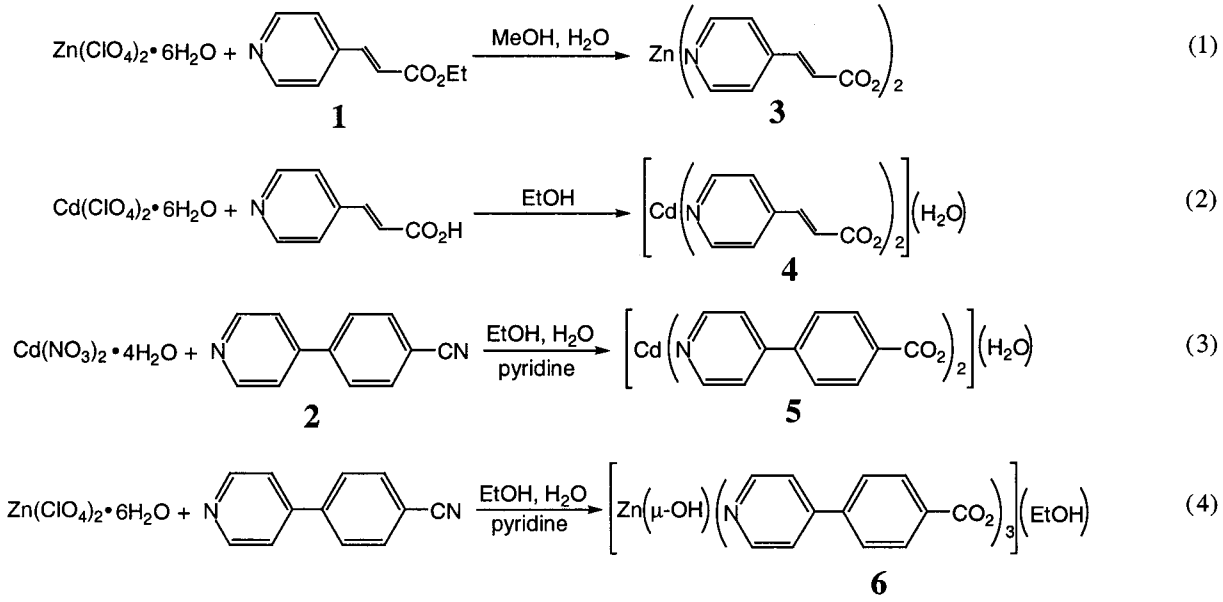

colorless crystals of dimensions of 0.06 × 0.08 × 0.54, 0.14 × 0.40 × 0.40, 0.12 × 0.16 × 0.28, and 0.14 × 0.24 × 0.24 mm, respectively. All of the structures were solved by direct methods. The structures of **3**, **4**, and **6** were refined on F^2 by full-matrix least squares using anisotropic displacement parameters for all non-hydrogen atoms.[12] Because of the large number of non-hydrogen atoms in the asymmetric unit of **5**, only Cd, O, and N atoms were refined on F^2 by full-matrix least squares using anisotropic displacement parameters, while all of the carbon atoms were refined isotropically. Compound **5** is enantiomerically twinned, and a TWIN card was used in the refinement to give a Flack parameter of 0.46-(3). All of the hydrogen atoms in **3** were located in electron density difference maps and refined isotropically, while all of the hydrogen atoms in **4**−**6** were located by geometric placing. No attempt has been made to locate hydrogen atoms on the guest molecules in **4**−**6**. Final refinement gave satisfactory *R* factors and goodness of fits for **3**−**6**. Experimental details for X-ray data collections of **3**-**6** are tabulated in Table 1, while selected bond distances and angles for **3**−**6** are listed in Table 2. All of the drawings were made using either XP[12] or CAMERON[13] programs.

Results

Synthesis. 1 was synthesized by a Heck coupling reaction between 4-bromopyridine and ethyl acrylate in 89% yield, while **2** was prepared by a Stille coupling reaction between 4-(trimethylstannyl)pyridine[11] and 4-bromobenzonitrile in 87% yield. **3** was obtained as colorless prismatic crystals in 35% yield by a hydro-(solvo)thermal reaction between $Zn(ClO_4)_2 \cdot 6H_2O$ and **1** in a mixture of methanol and water at 95 °C (eq 1 in Scheme 1), while **4** was synthesized in 53% yield by a hydro(solvo)thermal reaction between and 4-pyridylacrylic acid in ethanol at 130 °C (eq 2). **5** was prepared

(12) SHELX-TL, Version 5.1, Bruker Analytical X-ray Systems, Inc., Madison, WI, 1997.

(13) Watkin, D. J.; Prout, C. K.; Pearce, L. J. *CAMERON*; Chemical Crystallography Laboratory, University of Oxford: Oxford, U.K., 1996.

Table 2. Selected Bond Distances (Å) and Bond Angles (deg) for 3−6[a]

			3				
Zn1	O1	1.947(2)	Zn1	N2B	2.070(2)		
Zn1	O4	2.000(1)	Zn1	O3	2.484(3)		
Zn1	N1A	2.038(3)					
O1	Zn1	O4	111.0(1)	O4	Zn1	N1A	118.3(1)
O1	Zn1	N1A	115.4(1)	O4	Zn1	N2B	98.8(1)
O1	Zn1	N2B	110.3(1)	N1A	Zn1	N2B	100.8(1)
			4				
Cd1	O1	2.337(5)	Cd1	O4	2.277(6)		
Cd1	O2	2.351(5)	Cd1	N1A	2.268(6)		
Cd1	O3	2.436(6)	Cd1	N2B	2.263(7)		
O1	Cd1	O2	55.7(2)	O2	Cd1	N2B	87.5(3)
O1	Cd1	O3	152.6(3)	O3	Cd1	O4	54.9(3)
O1	Cd1	O4	100.2(3)	O3	Cd1	N1A	100.5(3)
O1	Cd1	N1A	90.6(2)	O3	Cd1	N2B	91.0(2)
O1	Cd1	N2B	110.7(2)	O4	Cd1	N1A	92.0(2)
O2	Cd1	O3	111.2(3)	O4	Cd1	N2B	144.8(3)
O2	Cd1	O4	96.6(2)	N1A	Cd1	N2B	103.8(3)
O2	Cd1	N1A	146.2(2)				
			5[b]				
Cd1	O4	2.209(8)	Cd3	O10	2.281(8)		
Cd1	O2	2.260(9)	Cd3	O12	2.305(9)		
Cd1	N3	2.274(9)	Cd3	N6C	2.334(10)		
Cd1	N4A	2.318(11)	Cd3	O11	2.411(11)		
Cd1	O1	2.619(9)	Cd3	O9	2.424(9)		
Cd3	N5B	2.260(10)					
O4	Cd1	O2	111.0(4)	O10	Cd3	O12	100.6(4)
O4	Cd1	N3	93.5(4)	O10	Cd3	N6C	90.9(3)
O2	Cd1	N3	136.8(3)	O12	Cd3	N6C	140.2(4)
O4	Cd1	N4A	128.3(4)	N5B	Cd3	O11	117.9(4)
O2	Cd1	N4A	93.4(4)	O10	Cd3	O11	105.1(4)
N3	Cd1	N4A	98.5(4)	O12	Cd3	O11	54.4(3)
O4	Cd1	O1	136.8(4)	N6C	Cd3	O11	85.8(3)
O2	Cd1	O1	53.9(3)	N5B	Cd3	O9	85.7(4)
N3	Cd1	O1	83.7(3)	O10	Cd3	O9	55.9(3)
N4A	Cd1	O1	94.6(4)	O12	Cd3	O9	90.6(3)
N5B	Cd3	O10	136.5(4)	N6C	Cd3	O9	126.3(3)
N5B	Cd3	O12	99.1(4)	O11	Cd3	O9	138.7(3)
N5B	Cd3	N6C	98.0(4)				
			6				
Zn1	O4	1.936(4)	Zn2	O7	1.925(4)		
Zn1	O7	1.945(4)	Zn2	O1	1.956(4)		
Zn1	O6	1.958(4)	Zn2	N2B	2.041(4)		
Zn1	N1A	2.053(4)	Zn2	N3C	2.036(4)		
O4	Zn1	O7	113.3(2)	O1	Zn2	O7	112.1(2)
O4	Zn1	O6	112.6(2)	O1	Zn2	N2B	98.3(2)
O7	Zn1	O6	111.6(2)	O1	Zn2	N3C	123.3(2)
O4	Zn1	N1A	113.0(2)	O7	Zn2	N2B	113.4(2)
O6	Zn1	N1A	97.0(2)	O7	Zn2	N3C	100.4(2)
O7	Zn1	N1A	108.0(2)	N2B	Zn2	N3C	109.9(2)

[a] Symmetry operations. **3**: A = −1 + *x*, 2 − *y*, *z* − 0.5; B = *x* − 0.5, 1.5 − *y*, *z* − 1.5. **4**: A = 1 + *x*, 2 − *y*, 0.5 + *z*; B = −*x* − 0.5, 1.5 − *y*, *z* − 1.5. **5**: A = 1 + *x*, *y*, *z*; B = *x*, 0.5 − *y*, 0.5 + *z*; C = −0.5 + *x*, 0.5 + *y*, 0.5 + *z*. **6**: A = *x*, −0.5 − *y*, *z* − 0.5; B = −*x*, 2 − *y*, 1 − *z*; C = 1 − *x*, 2 − *y*, 1 − *z*. [b] Cd2, Cd5, and Cd6 adopt coordination environments similar to that of Cd1, while Cd4 and Cd7 adopt coordination environments similar to that of Cd3.

by a hydro(solvo)thermal reaction between $Cd(NO_3)_2 \cdot 4H_2O$ and **2** in a mixture of ethanol, pyridine, and water in 65% yield at 140 °C (eq 3). However, when a similar reaction was carried out between $Zn(ClO_4)_2 \cdot 6H_2O$ and **2**, **6** was obtained in 44% yield (eq 4). The IR spectra of **3**−**6** clearly indicated the absence of the perchlorate and nitrate anions and the presence of carboxylate groups.[12] Furthermore, the symmetric carboxylate C═O stretch for **4** appears at 1400 cm^{-1}, while the symmetric carboxylate C═O stretches for **3** and **6** appear at 1371 and 1362 cm^{-1}, respectively. These symmetric carboxylate C═O stretching frequencies suggest that **4** possesses chelating carboxylate groups

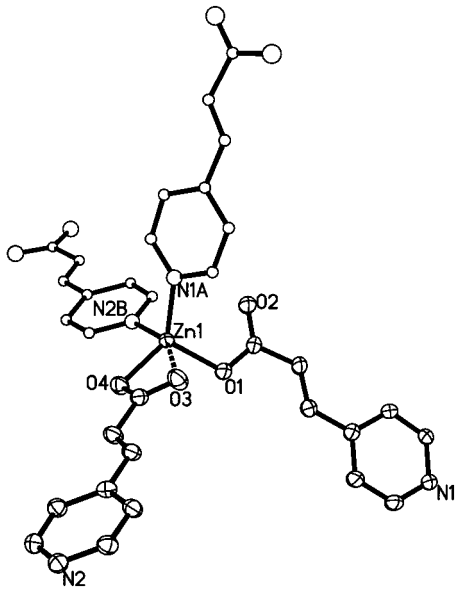

Figure 1. Coordination environment of **3**. The asymmetric unit is shown in ellipsoids at 50% probability. The open circles with increasing sizes represent C, N, and O, respectively.

while **3** and **6** contain monodentate carboxylate groups. The symmetric carboxylate C═O stretch for **5** appears as a very strong and broad peak at 1396 cm^{-1}, suggesting the presence of both monodentate and bidentate carboxylate groups. The formulation of compounds **3**−**6** has been supported by elemental analyses. The pyridinecarboxylate ligands in **3**, **5**, and **6** have evidently resulted from the in situ hydrolysis of **1** and **2** under reaction conditions, respectively. We have recently demonstrated the utility of such a "controlled release" of desired pyridinecarboxylate ligands via slow hydrolysis of their corresponding precursors in the synthesis of two- and three-dimensional coordination polymers.[7,15]

X-ray Single-Crystal Structure of 3. The polymeric structure of **3** was revealed by an X-ray single-crystal structure determination. **3** crystallizes in the acentric monoclinic space group *Cc*. Each asymmetric unit of **3** contains one Zn atom and two 4-pyridylacrylate groups. All of the atoms lie on general positions. The local coordination geometry around the Zn1 center can be described as a distorted tetrahedron. The Zn1 center coordinates to two pyridyl nitrogen atoms and two carboxylate oxygen atoms (O1 and O4) of four different 4-pyridylacrylate ligands (Figure 1). Although there is some interaction between the Zn1 and O3 atoms [with a Zn1−O3 separation of 2.484(3) Å], we consider the O3−C9−O4 carboxylate group to be monodendate and **3** to have a tetrahedral coordination geometry based on two factors. First, the angles around the Zn1 tetrahedron range from 98.8 to 118.3°, which only slightly deviate from those of a perfect tetrahedron. Second, the C9−O3 distance of 1.234(3) Å is consistent with the carbonyl character [the C1−O2 distance for the other monodentate carboxylate group is 1.242(4) Å].

(14) Mehrotra, R. C.; Bohra, R. *Metal Carboxylates*; Academic Press: New York, 1983.

(15) Lin, W.; Chapman, M. E.; Wang, Z.; Yee, G. T. *Inorg. Chem.* **2000**, *39*, 4169−4173. (b) Evans, O. R.; Wang, Z.; Lin, W. *Chem. Commun.* **1999**, 1903−1904. (c) Evans, O. R.; Wang, Z.; Xiong, R.-G.; Foxman, B. M.; Lin, W. *Inorg. Chem.* **1999**, *38*, 2969−2973.

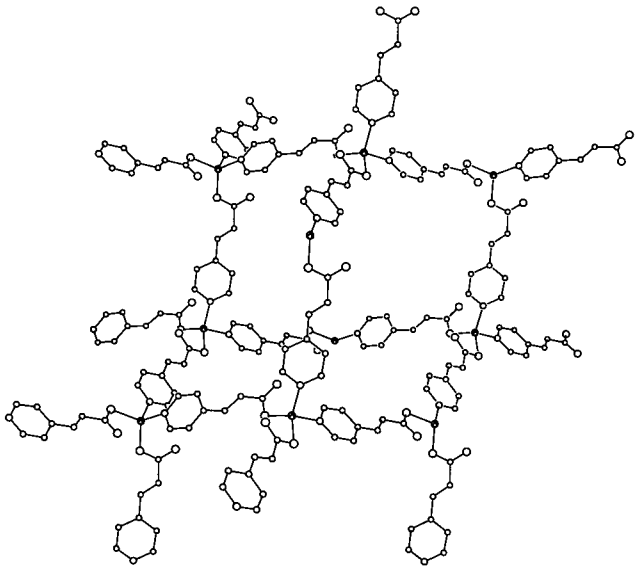

Figure 2. Diamondoid structure of **3**. The ellipsoids represent Zn atoms, while the open circles with increasing sizes represent C, N, and O atoms, respectively.

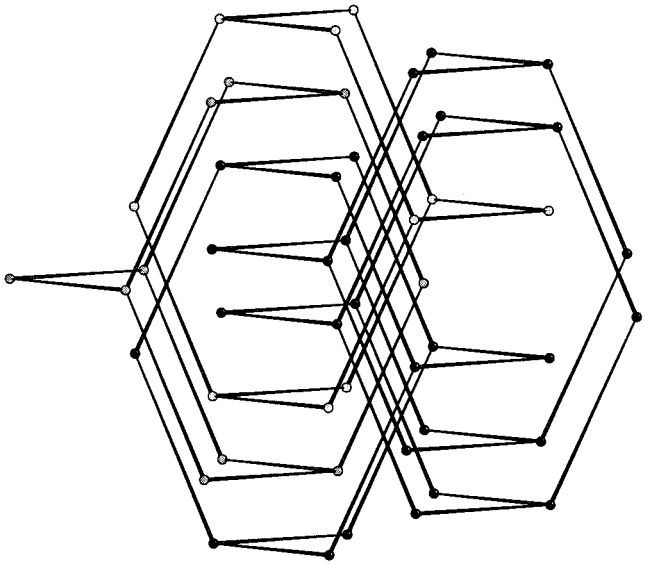

Figure 3. Diagram illustrating the 5-fold interpenetration in **3**. Only the Zn centers are shown.

The Zn1 center is connected to four adjacent Zn centers through the 4-pyridylacrylate bridges to result in a three-dimensional polymeric network with a diamondoid structure (Figure 2). The Zn−Zn separations are 10.92 and 11.23 Å within the diamondoid network. If the 4-pyridylacrylate bridges are omitted, the Zn−Zn−Zn angles within each diamondoid network in **3** range from 96.3 to 133.3°. These angles deviate significantly from 109.45° expected for an idealized diamond network, and each diamondoid network in **3** is thus highly distorted. With long Zn−Zn separations, very large cavities are formed within each diamondoid network in **3** (Figure 2). Compound **3** has effectively avoided the formation of a large void space via a 5-fold interpenetration (Figure 3), and, in fact, no solvent molecules have been included in **3**. Thermogravimetric analysis has confirmed the absence of included guest molecules in **3**; compound **3** shows no weight loss until the onset decomposition temperature of 360 °C.

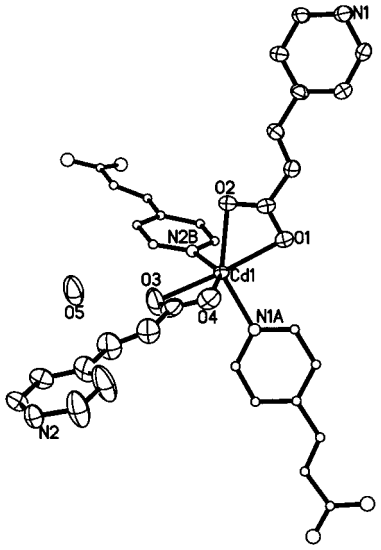

Figure 4. Coordination environment of **4**. The asymmetric unit is shown in ellipsoids at 50% probability. The open circles with increasing sizes represent C, N, and O, respectively.

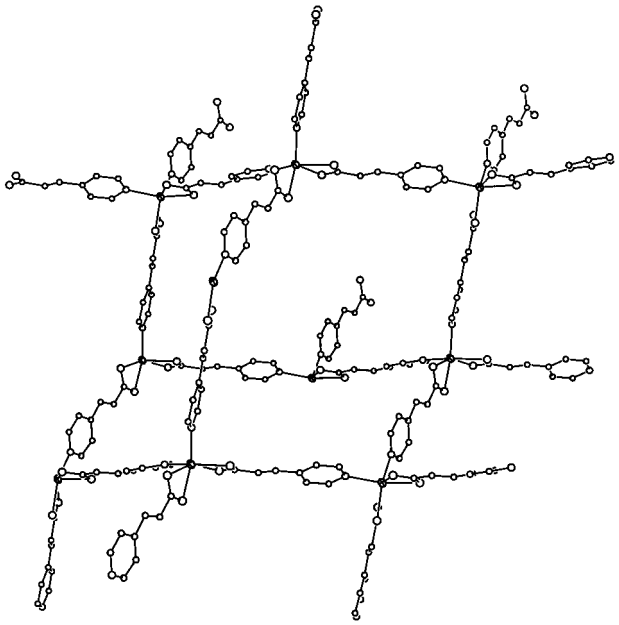

Figure 5. Diamondoid structure of **4**. The ellipsoids represent Cd atoms, while the open circles with increasing sizes represent C, N, and O atoms, respectively.

X-ray Single-Crystal Structure of 4. Compound **4** also crystallizes in acentric monoclinic space group *Cc*. The Cd centers in **4** adopt a highly distorted octahedral geometry by coordination to two pyridyl nitrogen atoms and to two carboxylate groups in a chelating fashion (Figure 4). Despite the difference in metal coordination environments, **4** exhibits a network topology very similar to that of compound **3** and also adopts a 5-fold diamondoid structure (Figure 5). Owing to larger Cd radii vs Zn radii, the Cd−Cd separations are slightly longer at 11.52 and 11.53 Å. As a consequence, **4** also includes a water guest molecule to occupy the extra space within the 5-fold interpenetrated diamondoid network. The presence of such open cavities in **4** after 5-fold interpenetration can be clearly seen from a space-filling model. The Cd−Cd−Cd angles range from 91.6 to 128.6° within each diamond net.

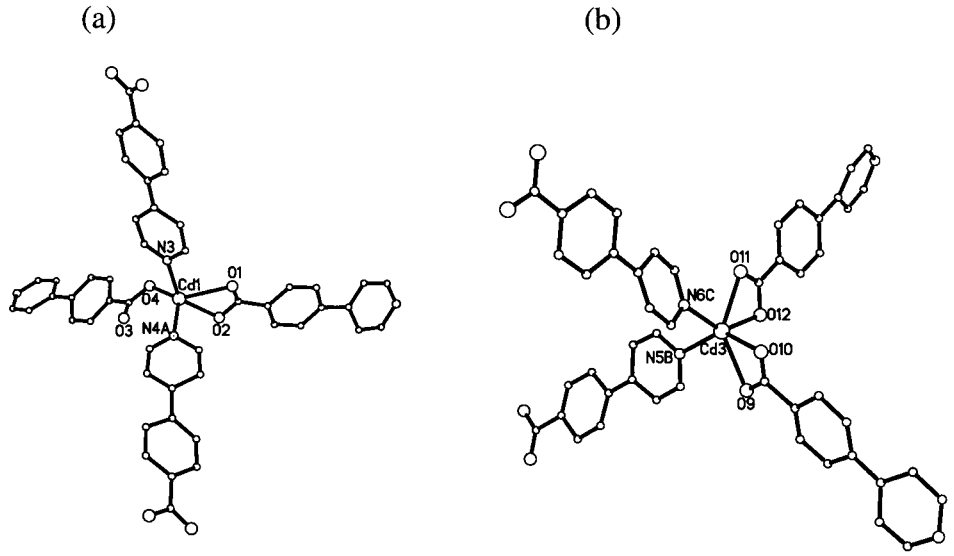

Figure 6. Coordination environments of (a) the Cd1 center and (b) the Cd3 center in **5**. The open circles with increasing sizes represent C, N, O, and Cd, respectively.

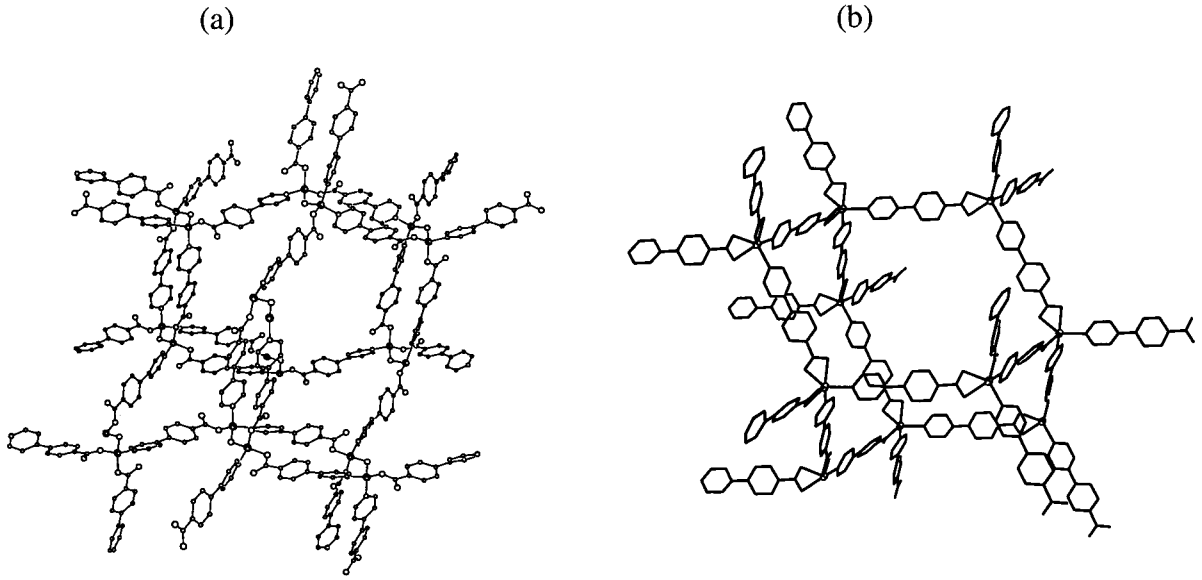

Figure 7. Diamondoid structure of **5** formed by (a) the Cd1 and Cd2 centers and (b) the Cd3 centers.

X-ray Single-Crystal Structure of 5. Compound **5** crystallizes in acentric monoclinic space group *Ia*. The asymmetric unit of **5** contains 7 Cd centers and 14 4-(4-pyridyl)benzoate ligands. We were only able to locate three water molecules in the asymmetric unit. There are two different coordination modes for the 4-(4-pyridyl)benzoate ligands: 10 of them adopt *exo*-tridendate linkage with chelating carboxylate groups, while the other four adopt *exo*-bidendate linkage with monodentate carboxylate groups. There are thus two different coordination environments for the Cd centers: the Cd1, Cd2, Cd5, and Cd6 centers adopt highly distorted trigonal-bipyramidal geometry by coordinating to two pyridyl nitrogen atoms and to one chelating carboxylate and one monodentate carboxylate group, while the Cd3, Cd4, and Cd7 centers adopt highly distorted octahedral geometry by coordinating to two pyridyl nitrogen atoms and to two chelating carboxylate groups (Figure 6).

Despite the different Cd coordination environments within the asymmetric unit, the Cd1 and Cd2 centers as well as the Cd5 and Cd6 centers are linked to each other to form 2-fold interpenetrated diamondoid networks, while the Cd3, Cd4, and Cd7 centers separately form three different diamondoid networks (Figure 7). Compound **5** thus adopts an overall 7-fold interpenetrated diamondoid structure (Figure 8). The Cd−Cd separations range from 13.45 to 13.64 Å, while the Cd−Cd−Cd angles range from 102.7 to 116.8° within each diamond net.

X-ray Single-Crystal Structure of 6. Compound **6** crystallizes in the monoclinic space group $P2_1/c$. Each asymmetric unit contains two Zn centers, one bridging hydroxyl group, three 4-(4-pyridyl)benzoate ligands, and one included ethanol molecule. Both Zn centers adopt distorted tetrahedral coordination geometry: the Zn1 center coordinates to two monodentate carboxylate groups, one pyridyl nitrogen atom, and one μ-OH group, while the Zn2 center coordinates to one monodentate carboxylate group, two pyridyl nitrogen atoms, and one μ-OH group (Figure 9). The bond angles around the Zn1 center range from 97.0(2) to 113.0(2)°, while those around the Zn2 center range from 98.3(2) to 123.3(2)°.

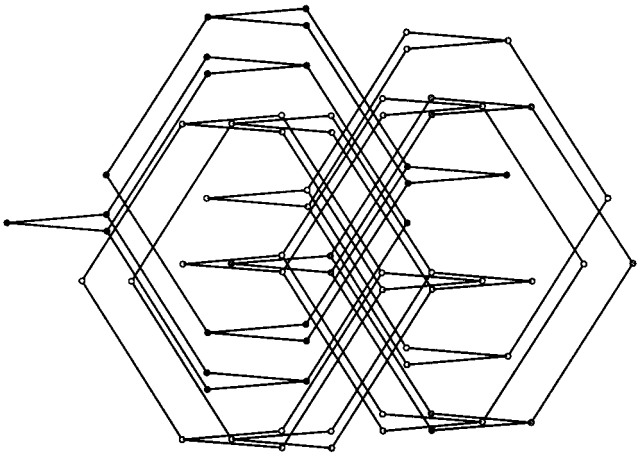

Figure 8. Diagram illustrating the 7-fold interpenetration in **5**. Only the Cd centers are shown.

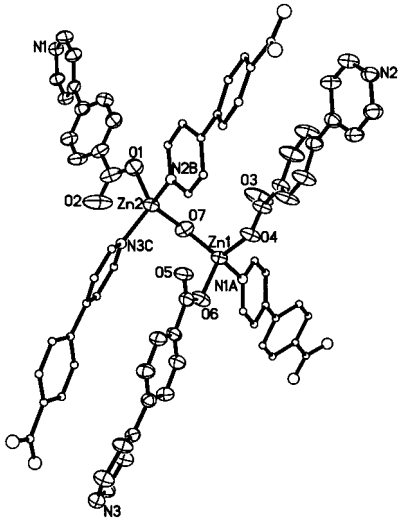

Figure 9. Coordination environment of **6**. The asymmetric unit is shown in ellipsoids at 50% probability. The open circles with increasing sizes represent C, N, and O, respectively. The included ethanol molecule has been omitted.

Interestingly, each $Zn_2(\mu\text{-OH})[4\text{-}(4\text{-pyridyl})\text{benzoate}]_3$ building unit is linked to four adjacent dizinc units to form a diamondoid coordination network (Figure 10). Two of the linkers are unsymmetrical 4-(4-pyridyl)-benzoate bridging ligands, while the other two linkers are symmetrical bis[4-(4-pyridyl)benzoate] double bridges. The two 4-(4-pyridyl)benzoate ligands within each double bridge are related by an inversion center, and thus each diamond net based on the $Zn_2(\mu\text{-OH})[4\text{-}(4\text{-pyridyl})\text{-benzoate}]_3$ building blocks is centrosymmetric. Because of the large separations between adjacent dizinc units, compound **6** adopts a 5-fold interpenetrated diamondoid structure to avoid the formation of very large open cavities. Even after the 5-fold interpenetration, some void spaces still exist in **6** and are clearly evident in a space-filling diagram (Figure 11). As a result, **6** also includes ethanol guest molecules to occupy the extra space within the 5-fold interpenetrated diamondoid network.

Powder Second Harmonic Generation Studies. We have carried out preliminary powder SHG studies using the 1064 nm fundamental wavelength from a Nd:YAG laser. Consistent with the single-crystal structures, compounds **3**−**5** are SHG-active. In contrast, compound

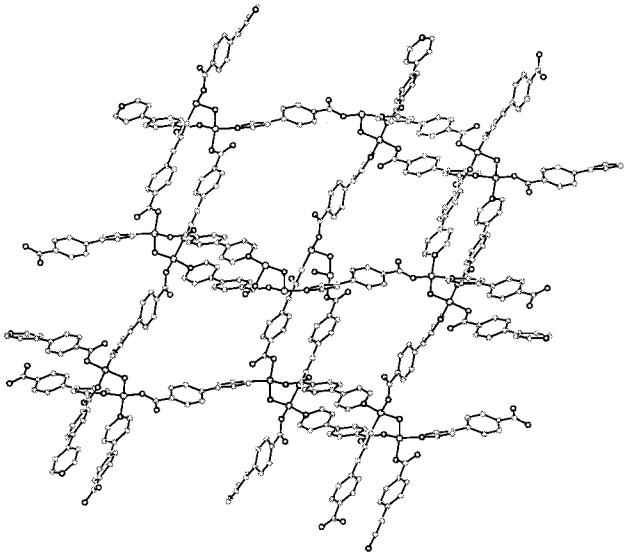

Figure 10. Diamondoid structure of **6**. The ellipsoids represent Zn atoms, while the open circles with increasing sizes represent C, N, and O atoms, respectively.

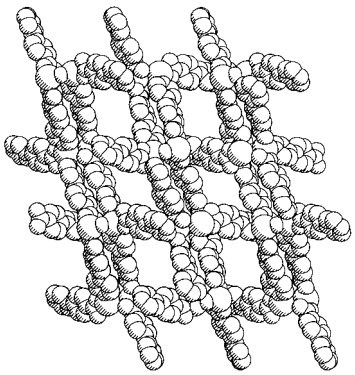

Figure 11. Space-filling model of **6** as viewed down the *b* axis. The open channels are occupied by removable ethanol molecules which have been omitted for clarity.

6 is SHG-inactive because of its centrosymmetric structure. **3** and **4** exhibit a powder SHG intensity of 126 and 18 relative to that of α-quartz, respectively, while **5** exhibits a powder SHG intensity of 310 relative to that of α-quartz. For comparison, technologically important lithium niobate has a powder SHG intensity of 600 relative to that of α-quartz. Because the SHG efficiency is proportional to the square root of the SHG intensity, compound **5** thus has nearly 80% of the SHG efficiency of lithium niobate. Given the relatively small electronic asymmetry in the 4-pyridylacrylate and 4-pyridylbenzoate chromophores, the powder SHG efficiencies observed here are quite respectable. Incorporation of more efficient chromophoric building blocks into metal−organic diamondoid networks should lead to acentric solids exhibiting much higher NLO activity. These results thus clearly illustrate the potential of the rational synthesis of highly NLO-active polar solids based on diamondoid structures.

Removal of Guest Molecules: TGA and XRPD Studies. X-ray single-crystal structures clearly indicate the presence of open channel compounds **4**−**6**, which are occupied by guest water and ethanol molecules, respectively. TGA measurements show that the guest molecules in **4**−**6** can be readily removed by heating in air (Figure 12). Alternatively, we have successfully removed

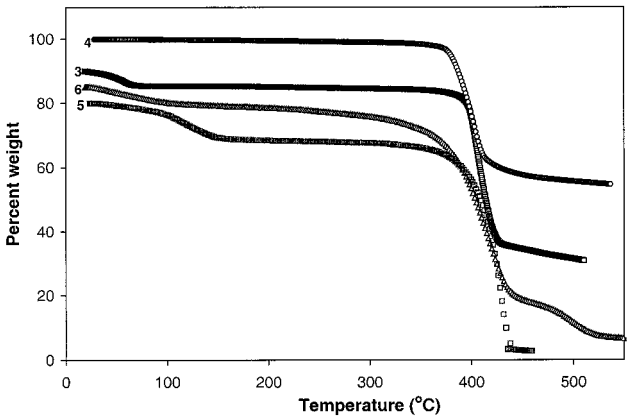

Figure 12. TGA curves for compounds **3**−**6**. For clarity, the curves for **3**, **5**, and **6** have been shifted down in percent weight.

these guest molecules by subjecting the ground samples of **4**−**6** to a 10^{-2} Torr vacuum for a few hours. XRPD patterns for the samples of **4** and **6** after removal of the included water and ethanol molecules remain essentially identical with those of pristine solids. TGA results indicate that the framework structures of compounds **4**−**6** are stable up to 380 °C. These results are consistent with our earlier observation that guest molecules within a 2-fold interpenetrated coordination network can be removed to generate a nanoporous material retaining the 2-fold diamondoid structure and conclusively demonstrate the framework stability of interpenetrated diamondoid coordination networks.

Discussion

Despite the very different metal coordination environments among compounds **3**, **4**, and **6**, they all form 5-fold interpenetrated diamondoid structures. The Zn1 center in **3** has a tetrahedral coordination geometry, while the Cd1 center in **4** adopts a distorted octahedral coordination environment. However, **3** and **4** have essentially identical network topology and crystallize in the same space group. Compound **5**, on the other hand, contains both 5- and 6-coordinated Cd centers, and yet adopts a 7-fold interpenetrated diamondoid network structure as a result of longer 4-(4-pyridyl)benzoate linking group vs 4-pyridylacrylate. More surprisingly, the $Zn_2(\mu\text{-OH})$-[4-(4-pyridyl)benzoate]$_3$ building units in **6** are also linked to each other via both mono[4-(4-pyridyl)benzoate] and bis[4-(4-pyridyl)benzoate] bridges to form a 5-fold interpenetrated diamondoid network. These results thus reinforce the notion that metal−organic coordination networks have a high tendency of adopting three-dimensional diamondoid structures. We believe that the ability of guest molecule inclusion as in compounds **4**−**6** provides additional flexibility in the packing of solids based on interpenetrated diamondoid structures. More importantly, these results strongly support our recent observations that the formation of diamondoid networks only depends on the connectivity of the neighboring metal centers (or bimetallic unit in **6**) but is not sensitive to the local coordination environment.

Diamondoid networks have long been recognized as promising structural motifs for the construction of acentric solids because diamondoid networks are not predisposed to pack in centric space groups owing to the lack of inversion centers on each tetrahedral connecting point. Many metal−organic diamondoid coordination networks have been synthesized prior to our work, but none of them have shown any second-order NLO activity. In fact, a low-temperature polymorph of KDP was the only NLO-active diamondoid network prior to our publication in 1999.[7a] The lack of NLO activity among the metal−organic coordination networks is simply a result of the biased choice of symmetrical bridging ligands with a single functional group (e.g., bipyridines and dicarboxylic acids). Construction of coordination polymers with multifunctional ligands is inherently more difficult owing to the different coordination ability of different functional groups (and often leading to the coordination of only one of the functional groups to the metal center). The use of symmetrical bridging ligands provides a source of centrosymmetry for each diamond net and tends to lead to centrosymmetric solids because of the dominance of dipole−dipole interactions. Our work has clearly indicated that unsymmetrical bifunctional bridging ligands are key to the construction of acentric diamondoid coordination networks. In fact, the centrosymmetric structure of **6** further shows that both bridging ligands should be unsymmetrical in order to guarantee the acentricity of each diamond net. Finally, the use of unsymmetrical, bifunctional bridging ligands (e.g., pyridinecarboxylates) is also necessary for the introduction of the electronic asymmetry (push−pull effects) that is essential for second-order optical nonlinearity.

We have also recently reported the synthesis of 8-fold diamondoid networks M{4-[2-(4-pyridyl)ethenyl]benzoate}$_2$ (M = Zn and Cd).[7d] Taken together, there is now compelling evidence that the degree of interpenetration can be readily controlled via the choice of bridging ligands of various lengths. With the appropriate linker length, an odd-number-fold metal−organic diamondoid network can be rationally synthesized, and for the first time an acentric solid can be crystal engineered. The present work thus highlights the potential of the rational synthesis of NLO materials based on interpenetrated diamondoid structures by combining transparent d^{10} metal centers and unsymmetrical bifunctional bridging ligands.

Acknowledgment. We acknowledge NSF (CHE-9875544) and ACS-PRF for financial support. We also thank Dr. Scott R. Wilson and the Materials Chemistry Laboratory at University of Illinois at Urbana−Champaign for X-ray data collections and Dr. I. Y. Chan for access to his laser. We thank Dr. R. Xiong for help with initial experiments and Dr. Y. Cui for help with the structure refinement of **5**. W.L. is an Alfred P. Sloan Fellow, an Arnold and Mabel Beckman Young Investigator, and a Cottrell Scholar of Research Corporation.

Supporting Information Available: Spectroscopic data for **1**−**6**: three figures and crystallographic information (PDF and CIF). This material is available free of charge via the Internet at http://pubs.acs.org.

CM010301N